Theory of Mn_{Ga}-H and other acceptor-H complexes in GaAs

J. P. Goss and P. R. Briddon
School of Natural Sciences, University of Newcastle upon Tyne, Newcastle upon Tyne, NE1 7RU, United Kingdom
(Received 23 June 2005; published 28 September 2005)

Mn doped GaAs is a potentially important material for the construction of dilute-ferromagnetic semiconducting devices. Due to the Mn ions representing both the magnetic ion and acceptor, the addition of hydrogen to selectively passivate Mn ions while retaining the magnetic properties has been suggested. However, the location of the H atom in the defect remains to be determined unambiguously. We present the results of density-functional calculations regarding the structure, vibrational and dilatation effects of X_{Ga} and X_{Ga}-H complexes for X=Mn, Be, Mg, and Zn. In all cases, H passivates the acceptor and energetically favors the bond-centered site. Passivated Mn_{Ga} is found to have a high-spin configuration of $S=5/2$.

DOI: 10.1103/PhysRevB.72.115211 PACS number(s): 61.72.Bb, 61.72.Vv, 71.20.Nr, 71.23.An

I. INTRODUCTION

Recent years have seen a huge effort in the development of dilute ferromagnetic semiconductors (DFS). Although theoretically wide-gap materials such as ZnO and GaN would give the highest Curie temperature (T_C), lying above room temperature for a hole concentration of 10^{18} cm^{-3}, effective p-type doping for these materials is a significant obstacle to the realization of this aim.

Perhaps the clearest results in III-V materials have been obtained for $Ga_xMn_{1-x}As$, since the Mn ions yield both the magnetic and p-type doping components. The acceptor level of Mn_{Ga} is around 0.11 eV above the valence band top,[1,2] and can be viewed as a $3d^5$ ion binding an effective-mass-like hole.[2–6]

However, the dual role of Mn may not be ideal since T_C depends both on the magnetic moments of the Mn^{2+} ion cores, and on the cube root of the hole density. It is viewed as advantageous to be able to independently control these two components. One mechanism suggested is codoping with additional acceptors, which has had some success.[7,8] However, this method may be frustrated by the solubility of Mn being strongly influenced by the Fermi level, so that the addition of Be, for example, increases the fraction of Mn ions that lie in the intersticies. The role of interstitial Mn may be to compensate the acceptors, but they have an uncertain effect on the ferromagnetic properties.[9–20] Additionally, there is an important contribution from small MnAs inclusions in the observed ferromagnetism.[21–23]

Although technical difficulties associated with codoping of GaAs with magnetic ions and acceptors may be overcome, an alternative method has been demonstrated in the past year where the DFS has been treated post growth with a source of hydrogen or deuterium.[24–27] The mechanism proposed is the passivation of the Mn_{Ga} acceptors by the formation of an intimate Mn_{Ga}-H or Mn_{Ga}-D pair, leading to a change in the hole concentration, but where the Mn ion retains the $S=5/2$ state, and hence the material retains magnetic properties, the passivated material becomes paramagnetic.

$Ga_xMn_{1-x}As$:H gives rise to a number of key observables that indicate the structure of the passivated Mn_{Ga}-H(D) complexes. The first is the frequency of an As-H stretch mode seen at low temperature in this material, reported at 2140.5–2142.2 cm^{-1} with x between 3.4% and 6% (Ref. 24) and 2143.0 cm^{-1} for similar material (Ref. 25). In deuterated material these modes shift to 1545–1545.9 cm^{-1} and 1546.5 cm^{-1} in the two reports. However, the location of the H or D is not clear, with the bond-centered (BC),[24] and antibonding to As site [AB(As)],[25] Fig. 1(b), viewed as likely candidates. For each case there is some basis for the assignment. In particular, Mn_{In} in InP traps hydrogen at a bond center.[28] However, antibonded hydrogen would be expected to give rise to a frequency weakly dependent on the acceptor species. Now, passivated Zn_{Ga} acceptors in GaAs have very similar H-related stretch modes at 2147 cm^{-1},[29,30] and are

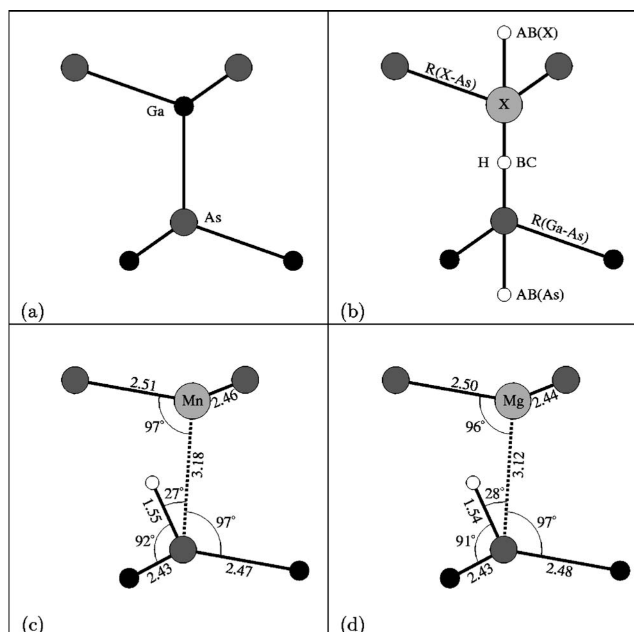

FIG. 1. Schematics of structures projected onto a (110) plane with the vertical and horizontal along [111] and $[1\bar{1}2]$ respectively. (a) is a section of bulk GaAs. (b) shows the on-axis bond-centered (BC) and two antibonding sites [AB(As) and AB(X)) for the substitutional X_{Ga} defect. (c) and (d) show the relaxed puckered Mn_{Ga}-H^*_{BC} and Mg_{Ga}-H^*_{BC} complexes, indicating distances (Å) and angles.

1098-0121/2005/72(11)/115211(8)/$23.00 ©2005 The American Physical Society

believed to be antibonding complexes.[25] A mode at a similar frequency ascribed in recent publications to Mg_{Ga}-H (Ref. 25) was only tentatively associated with Mg in early experiments,[29,30] and in fact corresponds to the Mn_{Ga}-H complex.[31] However, H passivation of Mg-doped GaAs shows clear results, indicating that some form of Mg_{Ga}-H centers exist.[32] In contrast to Zn_{Ga}-H, the Be_{Ga} acceptor is believed to trap H in the bond center, with the stretch modes at 2036.9 and 1471.2 cm^{-1} for H and D, respectively.[33,34]

The large difference in frequency of Mn_{Ga}-H relative to Be_{Ga}-H, and relative proximity to Zn_{Ga}-H might be viewed as lending weight to the antibonding assignment for Mn_{Ga}-H, Zn_{Ga}-H.[32] However, for Be and Zn theory suggests the bond centered or a slightly perturbed, off-axis site is most stable.[35–37] The experimental observations are inconclusive regarding the location of H, and an alternative model has been proposed[24,26,27] where it lies in the bond-centered location between Mn and one of its As neighbors, as shown schematically in Fig. 1(b).

In order to examine the impact of H/D on the electrical activity of Mn in GaAs, and to distinguish between the two likely models in Fig. 1, BC and AB(As), we have performed first principles calculations on the structure, local vibrational modes and dilatation of Mn_{Ga}, Mn_{Ga}-H and related structures in GaAs.

II. METHOD

We used local-spin-density-functional techniques in a supercell geometry as embodied in the code AIMPRO.[38] The Kohn-Sham functions are expanded in real space using a Gaussian basis set with four independent exponents centered at each atom site. For Be, Mg, Ga, and As three exponents are made up from independent *s* and *p* Gaussians, with the fourth exponent also containing *d* Gaussians. The Mn and Zn species are treated using four, *s*, *p*, and *d* Gaussian functions, and H by three independent *s* and *p* Gaussian functions. All species are treated using the pseudopotentials of Hartwigsen *et al.*,[39] with the Zn species including the 3*d* electrons explicitly in the valence. The charge density is Fourier transformed and expanded in plane waves with a energy cutoff of 300 Ry, this highly converged value being possible due to the use of a real-space Gaussian orbital basis for the Kohn-Sham functions. The experimental values of the GaAs bulk lattice constant and bulk modulus are reproduced in this theory to within 1%.

The Brillouin zone was sampled according to the Monkhorst-Pack scheme.[40] In general, relative energies were found to be converged to tens of meV using a $2\times2\times2$ (MP-2^3) mesh, but the relatively flat energy surfaces for a number of defects resulted in geometric differences between MP-2^3 and MP-4^3. For example, neutral, bond-centered interstitial hydrogen was found to be closer to As than Ga for MP-2^3, but equidistant from As and Ga with MP-4^3. However, even in these cases there was no structural change when the mesh was increased to MP-6^3, so we conclude that for structures MP-4^3 is sufficient.

Local vibrational modes (LVMs) are estimated by calculating the second derivatives of the total energy with respect to the ion positions for the core atoms, *viz.* X_{Ga}, the four As neighbors and the H atom. For all modes reported in this paper the Brillouin zone was sampled using MP-4^3; although we found that for many cases MP-2^3 gave indistinguishable results, for cases such as Be_{Ga}-H and particularly neutral H_{BC} there were noticeable shifts in H-related frequencies, and we therefore present the results for LVMs where all computational parameters are as close to each other as possible. The terms in the dynamical matrix due to the remaining atoms are approximated by a simple valence-force potential, which has a negligible effect on the high-frequency, H-related modes. Localization of LVMs on specific atoms is quantified by the length of the vector component of the normal modes associated with the atom. The calculated vibrational frequencies are quasiharmonic. Furthermore, the sensitivity of the stretch-mode frequency to the calculated bond lengths means that the error bars are of the order of a few percent.

Volume expansions were estimated by calculating the total energy for a given defect for a range of lattice constants. The volume displaced by the presence of the defect, ΔV is then defined as follows. For example, in a 64-atom supercell each defect is initially represented by a section of material with a volume $(2a_0)^3$, the volume that the cell would occupy in the absence of a defect. A similar quantity can be obtained for any supercell geometry. This defines V(bulk). We then calculate the total energy as a function of the lattice constant where the defect is present. In general the lattice constant which minimizes the total energy for the defect system differs from a_0 of bulk GaAs. The volume per cell containing the defect is V(defect), which for a 64-atom cell can be written as $(2a_0')^3$, where a_0' is the defect system lattice constant. Generally,

$$\Delta V = \frac{[V(\text{bulk}) - V(\text{defect})]}{(a_0^3/4)},$$

where $(a_0^3/4)$ is the volume per Ga—As pair in defect-free material. For the 64-atom cells used in this study, this reduces to $\Delta V=32[1-(a_0'/a_0)^3]$. ΔV is therefore a dimensionless quantity, and for a defect that exerts tensile or compressive strain on the surrounding material $\Delta V<0$ and $\Delta V>0$, respectively. The volume dilations were calculated using an MP-2^3 Brillouin-zone sampling. For a number of systems we checked the calculated values of ΔV using MP-4^3, and found only small differences. For example, the values for Be_{Ga}-H_{BC} the values were -0.065 and -0.058 for MP-2^3 and MP-4^3, respectively.

The majority of calculations have been performed in cubic supercells with side length $2a_0$ containing 64 host atoms, with convergence testing performed using 216 atom cubic cells of side length $3a_0$.

III. RESULT

A. Group-II acceptors in GaAs

We first report the structure and energetics of Mn_{Ga}, and compare these results with the well-known group-II acceptors, Be_{Ga}, Mg_{Ga}, and Zn_{Ga}.

TABLE I. Geometric parameters calculated for various acceptor and acceptor-hydrogen complexes in GaAs. Lengths are in Å, and angles in degrees. For all X_{Ga}, the X-As lengths are found to be independent of charge state. The X-H and H-As distances refer to those along the principle axis of the defects, and the X-As and As-Ga back-bonds lengths are those indicated in Fig. 1(b). Experimental (theoretical) bulk Ga-As bond lengths are 2.45 Å (Ref. 41) (2.43 Å, this study), and As-H bond lengths in arsine are 1.523 Å (Ref. 42) (1.52 Å, this study). Additionally, the ∠H-As-H of arsine is 92° and 91°, experimentally and theoretically, respectively. ΔV is the volume displaced by the defect, in units of $a_0^3/4$, the volume per Ga-As pair, and ΔE is the energy (eV) relative to that which we find to be most stable.

	Symmetry	ΔE	X-As	X-H	H-As	As-Ga	∠As-X-H	∠As-H-X	∠Ga-As-H	ΔV
Mn_{Ga}	T_d		2.51			2.41				0.18
Mn_{Ga}-H_{BC}	C_{3v}	0.0	2.46	1.92	1.52	2.43	94	180	102	0.35
Mn_{Ga}-H^*_{BC}	C_s	0.0	2.46, 2.51	1.90	1.55	2.43, 2.47	75, 111	131	92, 124	0.29
Mn_{Ga}-$H_{AB(As)}$	C_{3v}	0.2	2.53	4.28	1.64	2.44	114	0	80	0.25
Be_{Ga}	T_d		2.25			2.43				−0.33
Be_{Ga}-H_{BC}	C_{3v}	0.0	2.19	1.68	1.55	2.44	98	180	103	−0.07
Be_{Ga}-$H_{AB(As)}$	C_{3v}	0.6	2.19	4.53	1.54	2.48	99	0	75	−0.11
Mg_{Ga}	T_d		2.50			2.40				0.13
Mg_{Ga}-H_{BC}	C_{3v}	0.0	2.44	1.93	1.51	2.43	95	180	102	0.34
Mg_{Ga}-H^*_{BC}	C_s	0.0	2.44, 2.50	1.91	1.54	2.43, 2.48	74, 111	129	91, 125	0.29
Mg_{Ga}-$H_{AB(As)}$	C_{3v}	0.2	2.48	4.29	1.52	2.49	108	0	79	0.25
Zn_{Ga}	T_d		2.40			2.41				−0.07
Zn_{Ga}-H_{BC}	C_{3v}	0.0	2.36	1.81	1.53	2.43	96	180	102	0.18
Zn_{Ga}-$H_{AB(As)}$	C_{3v}	0.4	2.37	4.39	1.54	2.49	103	0	76	0.08
H^-_{BC}	C_{3v}	1.0	2.42	1.55	2.19	2.38	109	180	80	0.31
H^0_{BC}	C_{3v}	0.1	2.40	1.68	1.67	2.40	103	180	98	0.36
H^+_{BC}	C_{3v}	0.0	2.38	1.83	1.54	2.44	98	180	101	0.35
$H^-_{AB(As)}$	C_{3v}	0.6	2.49	4.33	1.73	2.41	116	0	81	−0.07
$H^0_{AB(As)}$	C_{3v}	0.0	2.44	4.31	1.67	2.45	110	0	77	0.11
$H^+_{AB(As)}$	C_{3v}	0.4	2.39	4.42	1.55	2.50	102	0	74	0.26
$H^-_{AB(Ga)}$	C_{3v}	0.0	2.42	1.69	4.52	2.41	87	0	115	−0.15
$H^0_{AB(Ga)}$	C_{3v}	0.1	2.43	1.92	4.43	2.44	74	0	111	0.03
$H^+_{AB(Ga)}$	C_{3v}	1.2	2.44	1.67	4.05	2.51	66	0	106	0.18
T^-_{As}	T_d	0.7		2.82	2.36					−0.13
T^0_{As}	T_d	0.1		2.82	2.41					0.04
T^+_{As}	T_d	1.3		2.84	2.39					0.14
T^-_{Ga}	T_d	0.1		2.24	2.87					−0.18
T^0_{Ga}	T_d	0.1		2.39	2.83					0.03
T^+_{Ga}	T_d	1.5		2.37	2.83					0.11

The Mn_{Ga} acceptor was relaxed with a range of effective spins in both the neutral and negative charge states. For Mn^-_{Ga}, we find that the $S=5/2$ spin state is most stable, with Mn_{Ga}-As internuclear distances of 2.51 Å, a modest dilation over the host bond length of around 3%. The geometric parameters are summarized in Table I. The large exchange interaction of the $3d$-electrons results in the $S=3/2$ and $7/2$ spin states lie 1.5 and 1.7 eV above the ground spin state. Mn^0_{Ga} is found to be most stable with $S=2$, corresponding to $Mn^-_{Ga}(\uparrow\uparrow\uparrow\uparrow\uparrow)+h^+(\downarrow)$, i.e., an antiferromagnetic interaction. Where the hole is aligned parallel to the $3d$ electrons, the energy is increased by around 0.2 eV. The antiferromagnetic interaction is in line with previous theory[3,12,43] and experiment.[44] As one would expect, the $(Mn_{Ga}\text{-As})^0$ bond-lengths are also 2.51 Å, consistent with the shallow nature of the hole.

The electrical levels of Mn_{Ga} can be estimated by comparison of the formation energies[45] for the neutral and negative charge states, or by comparison of the electron affinity of Mn_{Ga} with some system for which the acceptor level is known. We find that both procedures result in an acceptor level close to E_v, and are consistent with the $E_v+0.11$ eV obtained experimentally. Also consistent with experiment, the Mn_{Ga} acceptor level is calculated to be slightly deeper than those of the other acceptor species considered in this study.

B. Interstitial H in GaAs

The location of hydrogen in bulk GaAs has been studied theoretically previously.[35,36,46–49] In brief, these studies indicate that in the positive charge state H lies at a bond center, rather closer to the As neighbor than the Ga neighbor. The location of the H atom at the bond center in the positive charge state is also in agreement with muon spin relaxation experiments.[50] The site of the neutral species is less clear with different studies reporting the $H_{AB(As)}$ and H_{BC} sites, but with relatively little energy between them. The negative charge state locates H in a cage site (nonbonded). The different structures for different charge states renders the center negative-U, so that the neutral charge state is never thermodynamically more stable than the positive or negative forms.[49]

Table I lists the structural and energetic properties for various sites of interstitial H calculated using the method outlined above. The energetics and structures generally agree with the previous calculations, with the exception that we find that in the negative charge state the *T* site to be higher in energy than where a weak antibonding exists.

The activation energy for diffusion of hydrogen in *p*-type GaAs has been estimated theoretically to be around 0.5 eV,[49] corresponding to a path involving the *C* sites (midway between next-nearest-neighbor species), so that the activation energy is defined by the energy of hydrogen at the point approximately midway between two Ga atoms. This broadly agrees with the experimental value of ~0.66 eV obtained from capacitance transient measurements.[51] We have also simulated H lying close to the *C* sites for the positive charge state and find that, in contrast to the previous report, the C_{Ga} and C_{As} sites represent approximately the same barrier height, both lying around 0.45 eV above the bond-centered ground state. We note, however, that using a poorer Brillouin-zone sampling, such as the gamma-point approximation in Ref. 49, may lead to a difference in the activation energies.

C. Acceptor-hydrogen complexes

Armed with the agreement of our calculated properties of Mn_{Ga} and interstitial H with experiment and previous theory, we have some confidence in our ability to model hydrogenated acceptors.

The Mn_{Ga}-H complexes were initially relaxed subject to a C_{3v} symmetry constraint. In both the bond-centered and antibonding cases we find that the lowest energy spin state is $S=5/2$, in line with the experimental data. Indeed, the $S=1/2$, $S=3/2$, and $S=7/2$ spin states are around 3.4, 1.6, and 1.7 eV higher in energy, reflecting the excitation of valence electrons into the conduction band.

In all but the $S=1/2$ spin states we find that the lowest energy structure is that with H in the bond-centered location [Fig. 1(b)], and in particular the $S=5/2$ Mn_{Ga}-H_{BC} configuration is around 0.18 eV lower in energy than Mn_{Ga}-$H_{AB(As)}$. A trigonal structure with H antibonded to Mn was found to be around 0.84 eV higher in energy than Mn_{Ga}-H_{BC}, but only stable when the symmetry was constrained. Breaking the symmetry and re-relaxing results in the H atom reacting with a As-Mn bond. The resulting structure has practically the same total energy as the trigonal bond-centered case, but with the H-atom lying considerably off the [111] axis. The structure, labeled Mn_{Ga}-H^{*}_{BC}, is shown schematically in Fig. 1(c), and summarized in Table I. The similarity in energy between the on- and off-axis structures may be indicative of a rather flat energy surface, and the effective symmetry at elevated temperatures is likely to be axial.

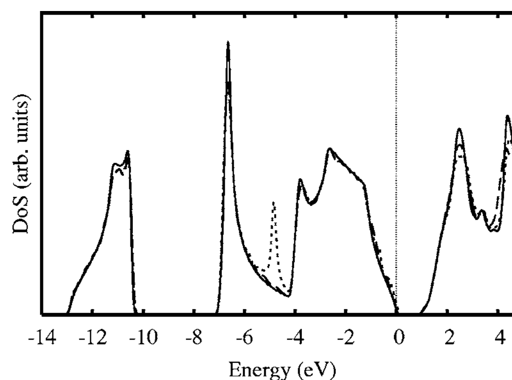

FIG. 2. Density of states for Mn_{Ga}-H in GaAs, with H lying at the bond-centered site. Dotted and dashed lines indicate the density of states for majority and minority spins, respectively, with the density of states of bulk GaAs, shown as a solid line. The zero energy is at the valence band top of bulk GaAs.

The electronic structure of the Mn_{Ga}-H complex is independent of the site of the H atom, with the band gap being free from any defect states, rendering the complex completely passive. Figure 2 shows the electronic density of states obtained by averaging over the Kohn-Sham eigenvalues for a uniform mesh in the Brillouin-zone made up from $20\times20\times20$ points, with each state broadened using a Gaussian of width 0.1 eV. The occupied $d^{\uparrow}$-states associated with the Mn ion are deep in the valence band (around −5 eV), and the corresponding empty $d^{\downarrow}$ states are high in the conduction band. This is in line with the electronic structure of Mn_{Ga}, and confirms the experimental picture of passivation presented previously.[24,25]

The calculated LVMs are listed in Table II. The bond-centered structure is predicted to yield a slightly higher frequency to the case with H antibonded to a neighboring As atom, but perhaps a more significant difference lies in low frequency bend modes, it might be through these that confidence could be gained for a specific atomic model. In particular, the resonance of an *E*-mode localized on Mn with the bend modes means that there are two sets of *E* bends (odd and even combinations), with the 305 cm^{-1} modes for Mn_{Ga}-D_{BC} having a particularly large amplitude on the Mn atom. These interactions are absent in the Mg_{Ga}-$H_{AB(As)}$ and Mg_{Ga}-$D_{AB(As)}$ cases. The off-axis structure also yields more bend-modes than the antibonded case, rendering these low frequency modes potentially critical to the correct structural assignment.

The differences in the LVMs of the bond-centered and antibonded geometries is small on the scale of the computed difference in the total energies, and we conclude that the

TABLE II. Hydrogen related local vibrational modes for X-H and X-D complexes in GaAs (cm^{-1}). All structures have C_{3v} symmetry except Mn_{Ga}-H^{*}_{BC} and Mg_{Ga}-H^{*}_{BC}, which are C_s due to the As-H bond lying off of the As-X internuclear direction. For C_{3v} centers there are a single, nondegenerate (A_1) stretch mode, and a pair of bend modes (E). For off-axis Mg-H structure, the stretch and bend modes are A' and (A',A''), respectively, with the lower frequency bend mode having A'' symmetry. The resonance with the Mn_{Ga} motion yields three H-related bend modes for Mn_{Ga}-H^{*}_{BC} with the lowest two having A'', and the higher A'.

	Bond-centered				Anti-bonded to As				Experiment	
	X-H		X-D		X-H		X-D			
X	Stretch	Bend	Stretch	Bend	Stretch	Bend	Stretch	Bend	X-H	X-D
Mn	2148	316, 289	1526	305, 278	1967	435	1401	324	2142[a]	1546[a]
Mn^{*}	1897	803, 343, 297	1349	579, 308, 277					2144[b]	1547[b]
Be	1954	335	1389	284	1937	458	1378	335	2037[c]	1471[c]
Mg	2242	283	1574	277	2003	424	1426	341		
Mg^{*}	1945	805, 405, 359	1384	585, 292						
Zn	2094	345,283	1488	296, 279	1930	440	1374	326	2147[b]	1549[b]
H^{+}	2016	321	1432	291	1904	342	1355	290		

[a]References 24 and 25, strained, low temperature.
[b]Reference 30, low strain, low temperature.
[c]Reference 33.

zero-point energy is unlikely to render the antibonded structure more stable.

For comparison, we relaxed Be_{Ga}, Mg_{Ga}, and Zn_{Ga} with H in the bond centered and two antibonding sites. The resultant structures are summarized in Table I. In *all* cases we find the bond-centered, or near-bond-centered location is the most stable. This broadly agrees with previous theoretical studies for Zn_{Ga}-H (Ref. 37) and Be_{Ga}-H (Refs. 35 and 52), but disagrees with the off-axis structure previously obtained for Zn_{Ga}-H.[36] Indeed, the off-axis structures of Mn_{Ga}-H^{*}_{BC} and Mg_{Ga}-H^{*}_{BC} are similar to that previously found for Zn_{Ga}-H_{BC}. However, despite using a range of starting structures we were unable to find a stable off-axis form for zinc. We also examined Zn_{Ga}-H in a larger supercell, and the results were found to closely follow those from the 64-atom calculations, with the energy difference between the Zn_{Ga}-H_{BC} and Zn_{Ga}-$H_{AB(As)}$ being within 10 meV of the value obtained in the 64-atom simulations (Table I).

We note that the bond lengths in the bond-centered Be_{Ga}-H complex differ slightly from those previously published,[35,52] with a shorter distance from the H atom to the Be acceptor, although the early reports were computationally lighter than those presented here. The results for Zn_{Ga}-H from Ref. 37 are close to those presented here, which is to be expected due to the similarity in approach.

Hydrogen antibonded to a neighboring As atom is metastable by 0.56, 0.17, and 0.44 eV higher for Be_{Ga}, Mg_{Ga}, and Zn_{Ga}, respectively. As with Mn_{Ga}, we find that hydrogen directly bonded to the acceptor species is always unstable, spontaneously reconstructing to an approximately bond-centered configuration in the absence of a symmetry constraint. We note that this result is at odds with the earlier theoretical result of Wang and Zhang[52] who found the H atom antibonded to Be was metastable and close in energy to the ground state. We note that in this earlier study the system was treated using a single k point at the zone center, which may have contributed to their result.

We have also examined structures where the H atom is removed by one site from the acceptor species, as suggested for Mg_{Ga}. These structures were generally structurally similar to isolated positively charged H_{BC}, but were higher in energy for all acceptors than when in a X-As bond, and are therefore ruled out on energetic grounds.

We find that all of the acceptor-hydrogen complexes were passive, as determined by examination of the band structure, and are bound with respect to isolated (charged) impurities. The reaction $A^{-}+H^{+}\rightarrow AH$ liberates 0.62, 0.64, 0.62, and 0.75 eV for Mn, Be, Mg, and Zn, respectively. Assuming that the activation energy for dissociation may be approximated by the sum of the binding energy and the migration barrier for H_{BC} (0.45–0.66 eV), these values can be compared directly with the experimental dissociation energies for Be, Mg, and Zn at 1.15 ± 0.10 eV, 0.9 ± 0.03 eV, and 1.36 ± 0.04 eV, respectively.[32,53,54] Given the crudeness of the estimate, the agreement is rather good.

Table II lists the calculated frequencies for H/D-related modes associated with Be, Mg, and Zn. In all hydrogenated cases we also find acceptor-related LVMs (Table III), and Be_{Ga} and Mg_{Ga} also have a sufficient mass difference from the host to give rise to LVMs, also listed in Table III. The calculated Be-related LVMs compare well with the experimental values of 482 cm^{-1} (Be_{Ga}), 555.7 cm^{-1} (Be_{Ga}-H), and 553.6 cm^{-1} (Be_{Ga}-D).[33,55] The bond-centered Be_{Ga}-H/D complexes yield Be-related modes in good agreement with the experimental modes, and reproduces an H/D splitting. The antibonded structure also has a Be-related mode which, although lying at 551 cm^{-1} is in agreement with the experiment, has a H/D splitting of <1 cm^{-1}, which we regard as additional support for the H_{BC} model.

The acceptor related modes for Mg are multiplied by the existence of three naturally occurring isotopes. Each gives

TABLE III. Local vibrational modes most strongly localized on the acceptor for X_{Ga} and X_{Ga}-H/D (cm^{-1}).

Defect	Sym	Frequencies(sym)		
		^{9}Be		
Be^{0}_{Ga}	(T_d)	467(T_2)		
Be^{-}_{Ga}	(T_d)	477(T_2)		
Be_{Ga}-H_{BC}	(C_{3v})	549(E)		
Be_{Ga}-D_{BC}	(C_{3v})	545(E)		
		^{24}Mg	^{25}Mg	^{26}Mg
Mg^{0}_{Ga}	(T_d)	313(T_2)	308(T_2)	304(T_2)
Mg^{-}_{Ga}	(T_d)	329(T_2)	324(T_2)	320(T_2)
Mg_{Ga}-H_{BC}	(C_{3v})	377(E)	371(E)	366(E)
Mg_{Ga}-D_{BC}	(C_{3v})	372(E)	367(E)	362(E)
Mg_{Ga}-H^{*}_{BC}	(C_s)	342(A')	337(A')	333(A')
		341(A')	336(A')	332(A')
Mg_{Ga}-D^{*}_{BC}	(C_s)	381(A'')	375(A'')	370(A'')
		^{55}Mn		
Mn^{0}_{Ga}	(T_d)	272(T_2)		
Mn^{-}_{Ga}	(T_d)	273(T_2)		
Mn_{Ga}-D_{BC}	(C_{3v})	305(E)		
Mn_{Ga}-H^{*}_{BC}	(C_s)	283(A')		
		283(A')		
Mn_{Ga}-D^{*}_{BC}	(C_s)	308(A'')		
		^{64}Zn	^{66}Zn	^{67}Zn
Zn_{Ga}-H_{BC}	(C_{3v})	284(E)	282(E)	281(E)

rise to a triply degenerate (T_2) mode, detailed in Table III. As with Be_{Ga}, the calculated frequencies for Mg_{Ga} are in good agreement with experiment[56] at 331, 325, and 321.5 cm^{-1} for the three Mg isotopes. In particular, the calculated isotope shifts are in excellent agreement. For Mg_{Ga}-D there is a resonance between the D bend and the Mg oscillation leading to an additional LVM with significant amplitude on both impurity species. There are no localized modes for Zn_{Ga}, but possibly one close to the one-phonon-maximum for Mn_{Ga}. Zn_{Ga}-related modes appear just above the one-phonon-maximum in Zn_{Ga}-H_{BC}, but are absent in the case of Zn_{Ga}-D_{BC} due to interaction with the deuterium-related bend modes.

In the case of the Mn center, the trigonal Mn_{Ga}-H_{BC} bend modes are coupled motion of H and Mn, in that the two E-modes represent odd and even combinations of E modes associated with the hydrogen and Mn, but with relatively little amplitude on Mn (~2%). The 305 cm^{-1} mode in the deuterium case shows a large (29%) amplitude on the Mn ion, and 51% on D. However, in the puckered cases, the 283 cm^{-1} A' mode is only weakly dependent on the H/D mass. It is 48% localized on Mn, and 85% localized over the group of Mn and its three As neighbors. The experimental observation of this mode would be key in determining the structure of the passivated complex.

D. Volume effects

The location of H in the defect may have a considerable effect on the effective volume occupied by the complex. It is generally assumed that the location of H in a cage or antibonding site will lead to a smaller displacement of volume, since there is not the substantial dilation of bonds associated with the bond-centered site.

We have calculated the volume displaced by each defect considered in this study, with the values listed in Table I. The trend follows intuition in that bond-centered H leads to a larger volume displacement than antibonded. Taking as an example, Mn_{Ga}-H, the volume displaced would give rise to an increase in the lattice constant proportional to the defect concentration,[57]

$$\delta a_0 \approx \frac{[X]}{[\mathrm{Ga}]}\frac{\Delta V}{3}a_0, \qquad (1)$$

where $[X]$ is the concentration of the defect, and [Ga] is the Ga-site density. Taking a typical Mn_{Ga} concentration of 10^{21} cm^{-3} in Eq. (1) yields numerically $\delta a_0 \approx 0.015 \times \Delta V$. The difference in δa_0 between puckered bond centered and antibonded to As is estimated at just $\sim 6 \times 10^{-4}$ Å.

IV. CONCLUSIONS

We have calculated the structure and properties of Mn_{Ga}, Mn_{Ga}-H and other acceptor species. In *all* cases the hydrogen passivates the acceptor, and is most energetically stable located at or close to a bond-centered site between the acceptor and an arsenic neighbor. The meV energy differences between on and off axis may not be significant, but in any case an off-axis structure may result in motional effects for all but very low temperature measurements, leading to observation of trigonal defects.

Overall agreement between the calculated and experimental vibrational modes for all acceptor-hydrogen complexes examined in this study is better for the bond-centered site than the antibonded, although the accuracy of the modes is not sufficient to be relied upon as a sole point of comparison with experiment. Additionally, the volume displaced by bond-centered and antibonded H is quite similar in the case of Mn_{Ga}-H, and it seems unlikely that such a measurement can be used to reliably predict the location of H.

The chief difference between the sites is that the low frequency ($270-900\ cm^{-1}$) modes, associated both with the acceptors and with hydrogen, are highly distinctive between structures, and would give a clear indication, if detected, as to the correct structure of the acceptor-hydrogen complex.

ACKNOWLEDGMENTS

This work was supported by the Engineering and Physical Sciences Research Council, UK. The authors gratefully acknowledge very helpful discussion with B. Clerjaud.

[1] W. Schairer and M. Schmidt, Phys. Rev. B **10**, 2501 (1974).
[2] M. Linnarsson, E. Janzén, B. Monemar, M. Kleverman, and A. Thilderkvist, Phys. Rev. B **55**, 6938 (1997).
[3] S. Sanvito, P. Ordejón, and N. A. Hill, Phys. Rev. B **63**, 165206 (2001).
[4] V. F. Sapega, M. Moreno, M. Ramsteiner, L. Däweritz, and K. Ploog, Phys. Rev. B **66**, 075217 (2002).
[5] P. Mahadevan and A. Zunger, Phys. Rev. B **69**, 115211 (2004).
[6] A. J. R. da Silva, A. Fazzio, R. R. dos Santos, and L. E. Oliveira, J. Phys.: Condens. Matter **16**, 8243 (2004).
[7] E. Johnston-Halperin, J. A. Schuller, C. S. Gallinat, T. C. Kreutz, R. C. Myers, R. K. Kawakami, H. Knotz, A. C. Gossard, and D. D. Awschalom, Phys. Rev. B **68**, 165328 (2003).
[8] D. Chiba, K. Takamura, F. Matsukura, and H. Ohno, Appl. Phys. Lett. **82**, 3020 (2003).
[9] K. M. Yu, W. Walukiewicz, T. Wojtowicz, I. Kuryliszyn, X. Liu, Y. Sasaki, and J. K. Furdyna, Phys. Rev. B **65**, 201303(R) (2002).
[10] S. C. Erwin and A. G. Petukhov, Phys. Rev. Lett. **89**, 227201 (2002).
[11] F. Máca and J. Mašek, Phys. Rev. B **65**, 235209 (2002).
[12] P. Mahadevan and A. Zunger, Phys. Rev. B **68**, 075202 (2003).
[13] F. Glas, G. Patriarche, L. Largeau, and A. Lemaître, Phys. Rev. Lett. **93**, 086107 (2004).
[14] K. W. Edmonds, P. Bogusławski, K. Y. Wang, R. P. Campion, S. N. Novikov, N. R. S. Farley, B. L. Gallagher, C. T. Foxon, M. Sawicki, T. Dietl, M. B. Nardelli, and J. Bernholc, Phys. Rev. Lett. **92**, 037201 (2004).
[15] M. Adell, J. Kanski, L. Ilver, J. Sadowski, V. Stanciu, and P. Svedlindh, Phys. Rev. Lett. **94**, 139701 (2005).
[16] K. W. Edmonds, P. Bogusławski, K. Y. Wang, R. P. Campion, S. N. Novikov, N. R. S. Farley, B. L. Gallagher, C. T. Foxon, M. Sawicki, T. Dietl, M. B. Nardelli, and J. Bernholc, Phys. Rev. Lett. **94**, 139702 (2005).
[17] B. J. Kirby, J. A. Borchers, J. J. Rhyne, K. V. O'Donovan, T. Wojtowicz, X. Liu, Z. Ge, S. Shen, and J. K. Furdyna, Appl. Phys. Lett. **86**, 072506 (2005).
[18] M. Malfait, J. Vanacken, V. V. Moshchalkov, W. Van Roy, and G. Borghs, Appl. Phys. Lett. **86**, 132501 (2005).
[19] D. Wu, D. J. Keavney, Ruqian Wu, E. Johnston-Halperin, D. D. Awschalom and Jing Shi, Phys. Rev. B **71**, 153310 (2005).
[20] K. M. Yu, W. Walukiewicz, T. Wojtowicz, J. Denlinger, M. A. Scarpulla, X. Liu, and J. K. Furdyna, Appl. Phys. Lett. **86**, 042102 (2005).
[21] M. Moreno, B. Jenichen, L. Däweritz, and K. H. Ploog, Appl. Phys. Lett. **86**, 161903 (2005).
[22] O. D. D. Couto, Jr., M. J. S. P. Brasil, F. Iikawa, C. Giles, C. Adriano, J. R. R. Bortoleto, M. A. A. Pudenzi, H. R. Gutierrez, and I. Danilov, Appl. Phys. Lett. **96**, 071906 (2005).
[23] M. Yokoyama, H. Yamaguchi, T. Ogawa, and M. Tanaka, J. Appl. Phys. **97**, 10D317 (2005).
[24] R. Bouanani-Rahbi, B. Clerjaud, B. Theys, A. Lemaitre, and F. Jomard, Physica B **340–342**, 284 (2003).
[25] M. S. Brandt, S. T. B. Goennenwein, T. A. Wassner, F. Kohl, A. Lehner, H. Huebl, T. Graf, M. Stutzmann, A. Koeder, W. Schoch, and A. Waag, Appl. Phys. Lett. **84**, 2277 (2004).
[26] S. T. B. Goennenwein, T. A. Wassner, H. Huebl, M. S. Brandt, J. B. Philipp, M. Opel, R. Gross, A. Koeder, W. Schoch, and A. Waag, Phys. Rev. Lett. **92**, 227202 (2004).
[27] A. Lemaître, L. Thevenard, M. Viret, L. Largeau, O. Maugin, B. Theys, F. Bernardot, R. Bouanani-Rahbi, B. Clerjaud, and F. Jomard, in *Proceedings of the 27th International Conference on the Physics of Semiconductors*, Vol. 772 of *AIP Conference Proceedings*, edited by J. Menéndez and C. G. Van de Walle (Springer-Verlag, Berlin, 2004), p. 363.
[28] B. Clerjaud, D. Côte, A. Lebkiri, and A. Mari, Mater. Sci. Forum **196–201**, 975 (1995).
[29] J. Chevallier, B. Clerjaud, and B. Pajot, in *Hydrogen in Semiconductors*, Vol. 34 of *Semiconductors and Semimetals*, edited by J. I. Panvoke and N. M. Johnson (Academic, San Diego, 1991), Chap. 13, pp. 447–510.
[30] B. Pajot, A. Jalil, J. Chevallier, and R. Azoulay, Semicond. Sci. Technol. **2**, 305 (1987).
[31] B. Clerjaud (private communication).
[32] M. C. Wagener, J. R. Botha, and A. W. R. Leitch, Phys. Rev. B **62**, 15315 (2000).
[33] P. S. Nandhra, R. C. Newman, R. Murray, B. Pajot, J. Chevallier, R. B. Beall, and J. J. Harris, Semicond. Sci. Technol. **3**, 356 (1988).
[34] M. Stavola, S. J. Pearton, J. Lopata, C. R. Abernathy, and K.

Bergman, Phys. Rev. B **39**, R8051 (1989).
[35] P. R. Briddon and R. Jones, Phys. Rev. Lett. **64**, 2535 (1990).
[36] A. Amore Bonapasta, M. Capizzi, and P. Giannozzi, Phys. Rev. B **57**, 12923 (1998).
[37] V. J. B. Torres, J. Coutinho, and P. R. Briddon, Comput. Mater. Sci. **33**, 145 (2005).
[38] R. Jones and P. R. Briddon, in *Identification of Defects in Semiconductors*, Vol. 51A of *Semiconductors and Semimetals*, edited by M. Stavola (Academic, Boston, 1998), Chap. 6.
[39] C. Hartwigsen, S. Goedecker, and J. Hutter, Phys. Rev. B **58**, 3641 (1998).
[40] H. J. Monkhorst and J. D. Pack, Phys. Rev. B **13**, 5188 (1976).
[41] J. Singh, *Physics of Semiconductors and their Heterostructures* (McGraw-Hill, New York, 1993).
[42] C. C. Loomis and M. W. P. Strinadberg, Phys. Rev. **81**, 798 (1951).
[43] R. Wu, Phys. Rev. Lett. **94**, 207201 (2005).
[44] V. F. Sapega, M. Moreno, M. Ramsteiner, L. Däweritz, and K. Ploog, Phys. Rev. Lett. **94**, 137401 (2005).
[45] S. B. Zhang and J. E. Northrup, Phys. Rev. Lett. **67**, 2339 (1991).
[46] L. Pavesi, P. Giannozzi, and F. K. Reinhart, Phys. Rev. B **42**, R1864 (1990).
[47] L. Pavesi and P. Giannozzi, Phys. Rev. B **46**, 4621 (1992).
[48] A. A. Bonapasta, M. Capizzi, and P. Giannozzi, Phys. Rev. B **59**, 4869 (1999).
[49] C. Wang and Q.-M. Zhang, Phys. Rev. B **59**, 4864 (1999).
[50] K. H. Chow, B. Hitti, R. F. Kiefl, R. L. Lichti, and S. F. J. Cox, Physica B **340–342**, 280 (2003).
[51] N. M. Johnson, C. Herring, and D. Bour, Phys. Rev. B **48**, R18308 (1993).
[52] C. Wang and Q.-M. Zhang, Phys. Rev. B **64**, 195204 (2001).
[53] S. J. Pearton, C. R. Abernathy, and J. Lopata, Appl. Phys. Lett. **59**, 3571 (1991).
[54] M. C. Wagener, J. R. Botha, and A. W. R. Leitch, Phys. Rev. B **60**, 1752 (1999).
[55] K. Laithwaite, R. C. Newman, and P. D. Greene, J. Phys. C **8**, L77 (1975).
[56] P. C. Leung, L. H. Skolnik, W. P. Allred and W. P. Spitzer, J. Appl. Phys. **43**, 4096 (1972).
[57] J. P. Goss, R. Jones, and P. R. Briddon, Phys. Rev. B **65**, 035203 (2002).